

Design, Synthesis, Cytotoxicity, and Docking Study of New Pyrano [3, 2-c] Pyridine - Based Derivatives

Safeya M. Mousa ^{1,*}, Eman S. Nossier ^{1, 2}, Aladdin M. Srouf ², Hanem M. Awad ³ and Heba S. A. Elzahabi ¹

¹ Department of Pharmaceutical Medicinal Chemistry and Drug Design, Faculty of Pharmacy (Girls), Al-Azhar University, Cairo, Egypt.

² Department of Therapeutic Chemistry, National Research Centre, Dokki, Giza, Egypt.

³ Department of Tanning Materials and Leather Technology, National Research Centre, Dokki, Giza, Egypt.

* Correspondence: dr.safya86@ymail.com

Article history: Received 2024-02-25

Revised 2024-03- 31-

Accepted 2024-05-04

Abstract: According to reports, pyrano[3,2-c]pyridine-based derivatives have promising anticancer properties and ability to hinder the binding to EGFR and VEGFR-2 tyrosine kinase receptors. Therefore, novel set of pyrano[3,2-c]pyridine 1-5 and pyrido[3',4':5,6]pyrano[2,3-d]pyrimidin-4-one **6** has been synthesized and constructed. Their chemical structures were confirmed *via* IR, ¹HNMR, ¹³CNMR, and mass spectra. Utilizing doxorubicin as a reference, all newly synthesized compounds were tested for their antitumor activity upon different kinds of cancer cells: colon carcinoma (HCT-116), hepatic carcinoma (HepG-2) and breast carcinoma (MCF-7). The antiproliferative results displayed that most derivatives had weak to moderate bioactivities on the examined cell lines. The formimidate **5** afforded the best cytotoxic activity contrary to all cell lines under test with IC₅₀ = 5.2 ± 0.1, 3.4 ± 0.3 and 1.4 ± 0.6 μM, in comparison to that of doxorubicin (IC₅₀ = 5.2 ± 0.30, 2.85 ± 0.4 and 1.03 ± 0.4 μM), respectively. To clarify binding ways and postulate technique of cytotoxicity, the promising hit **5** was also docked versus EGFR and VEGFR-2 kinases.

Keywords: Pyrano[3,2-c]pyridine; Anticancer; EGFR; VEGFR-2; Docking study.

This is an open access article distributed under the CC BY-NC-ND license <https://creativecommons.org/licenses/by/4.0/>

1. INTRODUCTION

Cancer is a global health problem and a big challenge for medical researchers. It is important that before designing a novel anticancer means to know molecular targets that is essential for replication and death of malignant cells ¹. So, it is essential to design targeted therapies in attempt to deliver drugs to specific genes or proteins that promote growth within cancer cells or tissues ². Epidermal growth factor (EGFR) and vascular endothelial growth factor receptor-2 (VEGFR-2) are important targets for many antitumor drugs ^{3,4}. Inhibition of EGFR is a familiar methodology in designing anticancer drugs as its signaling track has vital effect in the progression of many malignant tumors in addition to resistance to radiation and chemotherapy ⁵. Manipulations of EGFR are occurred by many abnormal proliferation and inflammatory diseases, including psoriasis, atherosclerosis, and many types

of tumors ⁶. Similarly, overexpression of VEGFR-2 mostly promoted the extent of benign tumors and its level was found to be rather high in cancers such as prostate, breast, ovarian, and colon carcinoma. Thus, inhibiting the VEGFR-2 signaling pathway reduces the growth of numerous cancer cell types, as well as angiogenesis ^{7,8}.

Compounds bearing pyran and pyridine scaffolds are considered interesting cores for a variety of pharmacological purposes as antimicrobial, antitubercular ^{9,10} and cytotoxic activity, through inhibition of EGFR, and VEGFR-2 ¹¹⁻¹³ (**Figure 1**). For example, the methylpyrano [2,3-c]pyrazole-5-carbonitrile derivative **I** ¹⁴ was reported as potent anticancer compound with higher activity than doxorubicin. Promising EGFR inhibitor pyrano[2,3-d]pyrimidine derivative **II** efficiently inhibited the EGFR enzyme with a significant IC₅₀ compared to lapatinib ¹⁵. Additionally, pyran and pyridine based derivatives were also reported to

Cite this article: Mousa SM., Eman S. Nossier ES., Srouf AM., Awad HM., Elzahabi HS. Design, Synthesis, Cytotoxicity, and Docking Study of New Pyrano [3, 2-c] Pyridine - Based Derivatives. Azhar International Journal of Pharmaceutical and Medical Sciences, 2025; 5 (2): 57- 65. doi: 10.21608/aijpm.2024.272713.1262

57

DOI : 10.21608/aijpm.2024.272713.1262

<https://aijpm.journals.ekb.eg/>

effectively inhibit VEGFR-2 enzyme. Sorafenib **III** bearing pyridine ring is a marketed anticancer drug with potent VEGFR inhibitory activity¹⁶. Pyridine based derivative **IV** exhibited nearly equipotent suppressing activity to sorafenib against VEGFR-2 with IC_{50} =65.83 and 61.65 nM, respectively¹⁷.

Using molecular hybridization and substituent variation techniques, a novel series of pyrano [3,2-*c*]pyridine **1-6** was designed and synthesized on the basis of the pharmacophoric characteristics of the

identified anticancer pyran (**I**, **II**) and pyridine compounds (**III**, **IV**). (**Figure2**). The antiproliferative effectiveness of these synthesized derivatives was screened alongside a panel of cancer cell lines including HCT-116, HepG-2, and MCF-7. To identify their way of action, the intriguing compound was further evaluated to determine its interactions and binding affinities within the selected enzymes EGFR and VEGFR-2 to get ideal lead for future improvement.

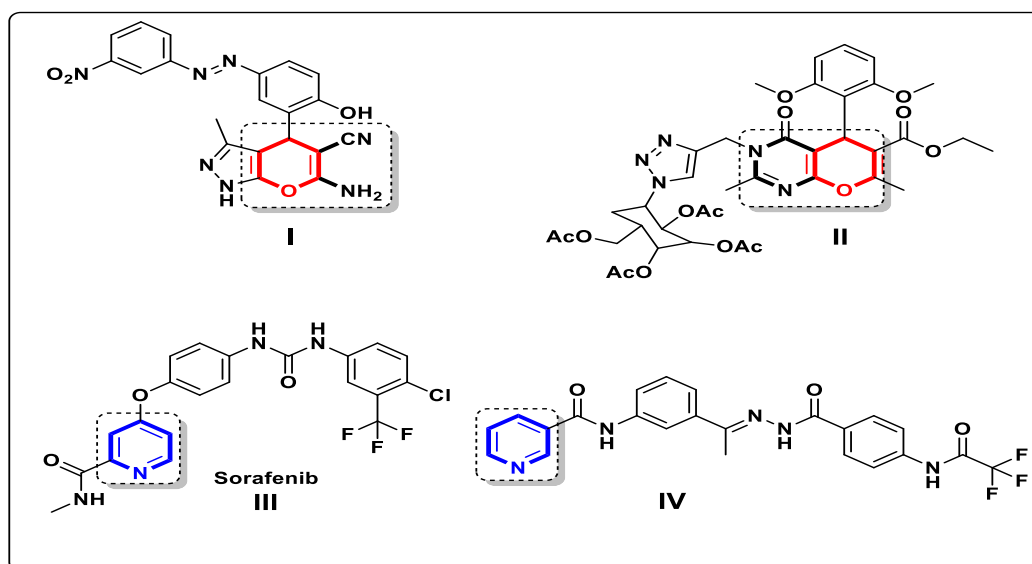


Figure1. Some reported pyran and pyridine scaffolds as anticancer agents^{1, 14-17}.

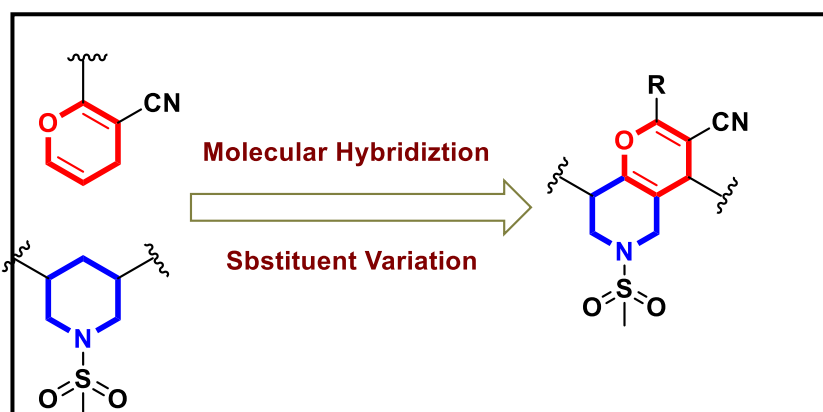


Figure2. Design and rationale for synthesis of new pyrano[3,2-*c*]pyridine based derivatives **1-5** and pyrano[2,3-*d*]pyrimidin-4-one **6**.

2. METHODS

2.1 Chemistry

Supplemental file contained all relevant information on the substances utilized and the various analytical instruments. The starting compounds

3,5-bis[4-chlorobenzylidene]-1-(methylsulfonyl) piperidin-4-one **A** and 4*H*-pyrano[3,2-*c*]pyridine-3

carbonitrile derivatives **B** were prepared as reported^[12,13]. All microanalytical and spectroscopic results are listed in table 1.

Table 1. Microanalytical and spectroscopic results of compounds 1-6.

Cpd	Yield %	m.p. ^o C	Color	IR (KBr) (cm ⁻¹)	¹ H-NMR (DMSO- <i>d</i> ₆) δ (ppm)	¹³ C-NMR (DMSO- <i>d</i> ₆) δ (ppm)	Analysis %	MS m/z (%)
1	65	240-2 43	white	2111 (CN), 1742 (CO)	2.25 (s, 3H, CH ₃), 3.90 (q, 1H, upfield H of piperidinyl H ₂ C-2"), 4.15 (dd, 1H, upfield H of piperidinyl H ₂ C-6"), 4.50 (d, 1H, downfield H of piperidinyl H ₂ C-2"), 5.10 (d, 1H, downfield H of piperidinyl H ₂ C-6"), 7.32 (d, 3H, CH=C, Ar-H), 7.40-7.48 (q, 4H, Ar-H), 7.53 (d, 2H,	36.08 (CH ₃), 45.50 (piperidinyl H ₂ C-2"), 46.94 (piperidinyl H ₂ C-6"), 126.14 (CN), 126.78, 127.82, 128.45, 1284.70, 131.20, 131.72, 133.12, 133.20, 140.09 & 153.52 (18 Ar-C) 169.13 (C=O)	C ₂₃ H ₁₆ Cl ₂ N ₂ O ₄ S (487.36) Calcd. (Found) C, 56.68 (56.72), H, 3.31 (3.54), N, 5.75 (5.89)	486.27 (24.07, M ⁺), 489.13 (15.30, M ⁺), 422.75 (100).
2	63	-200 202	green	3414 (NH), 2218 (CN), 1612 (C=O)	1.75 (s, 6H, 2Ph-CH ₃), 2.12 (s, 3H, COCH ₃), 2.29 (s, 3H, SO ₂ CH ₃), 3.51 (s, 1H, NH, exchangeable with D ₂ O), 3.61 (s, 2H, piperidinyl H ₂ C-2"), 4.11 (s, 1H, pyranyl-H), 4.54 (s, 1H, upfield H of piperidinyl H ₂ C-6"), 4.58 (s, 1H, downfield H of piperidinyl H ₂ C-6"), 6.66 (s, 1H, olefinic CH), 7.28 (s, 4H, Ar-H), 8.14 (s, 4H, Ar-H)	-	C ₂₇ H ₂₇ N ₃ O ₄ S (489.59) Calcd. (Found) C, 66.24 (66.51), H, 5.56 (5.82), N, 8.58 (8.63)	490.28 (37.08, M ⁺), 154.52 (100).
3	40	115-1 17	pale green powder	3444 (NH), 2210 (CN), 1685 (C=O)	2.33 (s, 6H, 2CH ₃), 2.84 (s, 3H, SO ₂ CH ₃), 2.94 (s, 2H, CH ₂ Cl), 4.01 (s, 2H, piperidinyl H ₂ C-2"), 4.26 (s, 1H, pyranyl-H), 4.47 (s, 2H, piperidinyl H ₂ C-6"), 6.94 (s, 1H, NH, D ₂ O exchangeable), 7.20-7.59 (m, 9H, Ar-H + olefinic CH)	-	C ₂₇ H ₂₆ ClN ₃ O ₄ S (523.13) Calcd. (Found) C, 61.88 (62.01), H, 5.00 (5.31), N, 8.02 (8.21)	523.86 (16.32, M ⁺), 365.27 (100).
4	55	230-2 32	brown	2210 (CN)	2.33 (s, 6H, N(CH ₃) ₂), 3.00 (s, 3H, SO ₂ CH ₃), 3.08, 3.10 (2s, 6H, ph-CH ₃), 4.00-4.50 (m, 4H, piperidinyl H ₂ C), 3.18 (s, 1H, pyranyl-H), 7.33-7.42 (m, 7H, Ar-H + olefinic CH), 8.02 (d, 2H, J= 7.2 Hz, Ar-H), 8.73 (s, 1H, olefinic CH)	-	C ₂₈ H ₃₀ N ₄ O ₃ S (502.63) Calcd. (Found) C, 66.91 (67.21), H, 6.02 (6.30), N, 11.15 (11.28)	503.72 (14.44, M ⁺), 395.37 (100).
5	48	300-3 02	brown	2210 (CN)	1.17 (t, 3H, CH ₃), 2.36 (d, 2H, piperidinyl H ₂ C-2"), 2.38 (d, 2H, piperidinyl H ₂ C-6"), 2.40 (s, 6H, 2Ph-CH ₃), 2.70 (q, 2H, CH ₂), 3.00 (s, 3H, SO ₂ CH ₃), 3.74 (s, 1H, pyranyl-H), 7.03- 7.70 (m, 9H, Ar-H + olefinic CH), 8.22- (s, 1H, olefinic CH)	-	C ₂₈ H ₂₉ N ₃ O ₄ S (503.62) Calcd. (Found) C, 66.78 (66.92), H, 5.80 (6.06), N, 8.34 (8.58)	504.07 (29.21, M ⁺), 115.42 (100)
6	58	280-2 82	brown	3333 (NH), 1647 (C=O)	1.03, 1.23 (2s, 6H, 2-PhCH ₃), 2.31 (s, 3H, SO ₂ CH ₃), 3.30 (s, 2H, piperidinyl H ₂ C) 4.03 (s, 2H piperidinyl H ₂ C), 4.50 (s, 1H, pyranyl-H), 5.1 (s, 1H, NH, D ₂ O exchangeable), 7.05 (s, 1H, olefinic CH), 7.09 (s, 1H, olefinic CH), 8.17-8.33 (m, 8H, Ar-H)	21.92 (2-PhCH ₃), 43.68 (SO ₂ CH ₃), 60.09 (CH ₂), 61.71 (CH ₂), 68.29 (CH-pyrane), (Ar-C), 161.48 (C=O)	C ₂₆ H ₂₅ N ₃ O ₄ S (475.56) Calcd. (Found) C, 65.67 (65.92), H, 5.30 (5.62), N, 8.84 (9.13)	476 (30.05, M ⁺), 327.30 (100).

2.1.1. 8-(4-Chlorobenzylidene)-4-(4-chlorophenyl)-6-(methylsulfonyl)-2-oxo-5,6,7,8-tetrahydro-2H-pyranopyridine-3-carbonitrile (1)

A mixture of compound **A** (10 mmol) in *n*-butanol (10 ml), ethyl cyanoacetate (10 mmol) in presence of little droplets of TEA was boiled for 4h. The formed precipitate underwent filtration and crystallization from ethyl alcohol producing **1**.

2.1.2 *N*-(3-Cyano-8-(4-methylbenzylidene)-6-(methylsulfonyl)-4-(*p*-tolyl)-5,6,7,8-tetrahydro-4H-pyranopyridin-2-yl)acetamide (2)

To prepare compound **2**, mixture of **B** (10 mmol) in acetic anhydride (20 ml) was heated for 3 h, after completion of reaction it was discharged over frozen water, then the separated residue was reassembled from ethanol.

2.1.3 Chloro-*N*-(3-cyano-8-(4-methylbenzylidene)-6-(methylsulfonyl)-4-(*p*-tolyl)-5,6,7,8-tetrahydro-4H-pyranopyridin-2-yl)acetamide (3)

A solution containing equimolar quantities of **B** and chloroacetyl chloride (10 mmol) was heated up in acetic acid for 5 h before being dumped over ice/water, and the detached particles were dried and reconstructed from ethyl alcohol to yield **3**.

2.1.4 *N'*-(3-cyano-8-(4-methylbenzylidene)-6-(methylsulfonyl)-4-(*p*-tolyl)-5,6,7,8-tetrahydro-4H-pyranopyridin-2-yl)-*N,N*-dimethylformimidamide (4)

An equimolar amounts of **B** and DMFDMA (10 mmol) were refluxed in dry xylene for 8h. The resulting compound was recovered via sifting and reformed from ethyl alcohol to yield **4**.

2.1.5 Ethyl-*N*-(3-cyano-8-(4-methylbenzylidene)-6-(methylsulfonyl)-4-(*p*-tolyl)-5,6,7,8-tetrahydro-4H-pyranopyridin-2-yl)formimidate (5):

A combination of equimolar quantities (10 mmol) of **B** and triethyl orthoformate (10ml) has been heated

for 7h. The reaction mixture was cooled to ambient temperature, dispensed onto frigid water and the resulting product was recrystallized from ethanol producing **5**.

2.1.6 9-(4-Methylbenzylidene)-7-(methylsulfonyl)-5-(*p*-tolyl)-3,5,6,7,8,9-hexahydro-4Hpyrido[3',4':5,6]pyranopyrimidin-4-one (6)

A suspension of **B** (10 mmol) in formic acid (10ml) was boiled for 7h then, rested to ambient temperature and mixed with cold water forming compact mass which gathered and reconstituted from ethyl alcohol to give **6**.

2.2 *In vitro* cytotoxic activity

In vitro anticancer ability was determined using MTT assay technique¹⁴ as explained in Supplemental data.

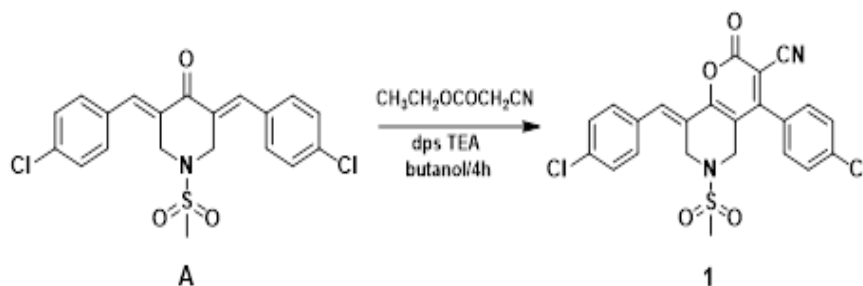
2.3 Docking studies

Modeling of the most promising compound **5** was accomplished against EGFR and VEGFR-2 ((PDB IDs: 1M17 and 4ASD, respectively) using MOE 14.0 program as mentioned in Supporting material¹⁵.

3. RESULTS and DISCUSSION

3.1 Chemistry

In **scheme 1**, 2H-pyranopyridine-3-carbonitrile derivative **1** has been obtained by the reaction of the starting compound 3,5-bis(4-chlorobenzylidene)-1-(methylsulfonyl)pyridin-4-one **A** and ethyl cyanoacetate according to the postulated pathway (**figure 3**).



Scheme 1. The synthetic route of pyranopyridine-3-carbonitrile **1**.

Additionally, compound **2** was prepared through N-acetylation of the NH₂ in the starting compound **B** with acetic anhydride. Compound **3** was obtained via interaction between **B** and chloroacetyl chloride in acetic acid under reflux. Synthesis of amidine bearing compound **4** occurred by refluxing of **B** and DMFDMA in dry xylene.

Formimidate derivative **5** was obtained by reacting **B** with triethyl orthoformate in the existence of acetic anhydride. Compound **6** was prepared via cyclo condensation of **B** using formic acid as reacting agents and solvent under reflux condition as observed in **scheme 2**.

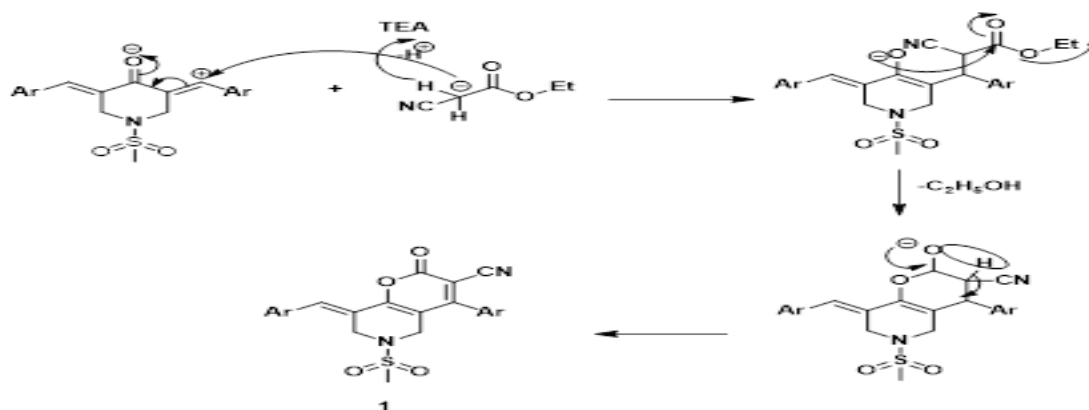
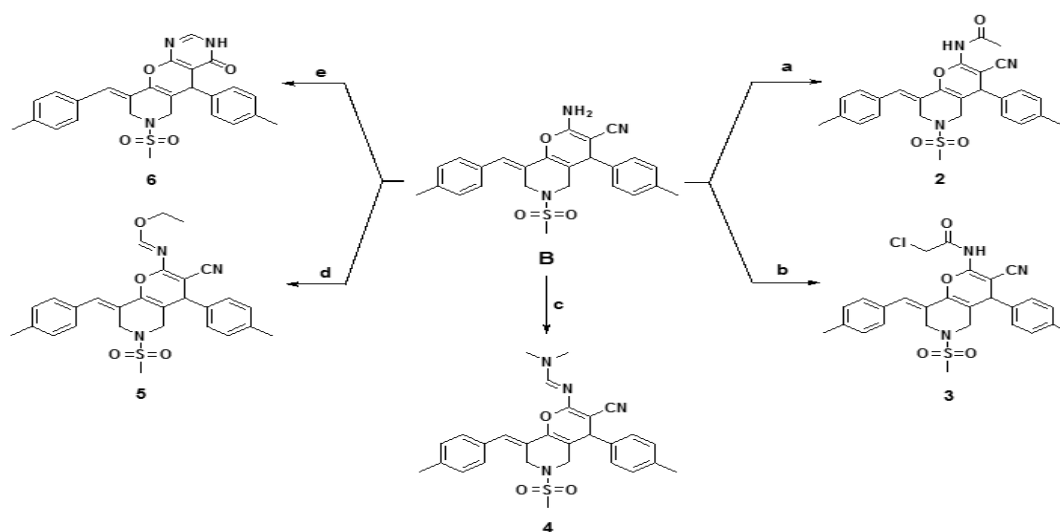


Figure 3. Proposed mechanism for synthesis of compound **1** from compound **A** and ethyl cyanoacetate in presence of TEA.



Reagents and conditions: (a) $\text{CH}_3\text{COOCOCH}_3$, reflux 3h; (b) ClCOCH_2Cl , AcOH, reflux 5h; (c) DMF-DMA, dry xylene, reflux 8h; (d) $\text{HC}(\text{O})_3(\text{CH}_2\text{CH}_3)_3$, reflux 7h; (e) HCOOH , reflux 7h

Scheme 2. The synthetic route of pyrano[3,2-*c*]pyridine derivatives **2-5** and pyrano[2,3-*d*]pyrimidin-4-one **6**.

Structures of **1-6** have been identified from their microanalytical and spectroscopic results. **IR** spectrum of **1** demonstrated bands at 2111 and 1742 for CN and CO cm^{-1} respectively. Also, $^{13}\text{C-NMR}$ spectrum confirmed the existence of two signals at δ 45.50 and 46.94 for (2 piperidinyl H_2C), and two characteristic signals assigned for CN and CO at 126.14 and 169.13 ppm respectively. In addition to that, $^1\text{H-NMR}$ (DMSO- d_6) spectrum of **2** presented a singlet signal at δ 1.75 ppm for the protons of two methyl groups in *p*- CH_3 phenyl rings. Also, another singlet was revealed at δ 2.12 ppm for acetyl protons. **IR** scale of **3** exhibited bands at 3444, 2210 and 1685 cm^{-1} for NH, CN and CO, respectively. $^1\text{H-NMR}$ (DMSO- d_6) spectrum of **3** represented three signals at δ 2.33, 2.84 and 2.94 ppm for the protons of two *p*- CH_3 phenyl rings, methyl sulfonyl protons and methylene chloride protons, respectively. **IR** spectrum of **4** indicated band at 2210 cm^{-1} due to presence of CN group. $^1\text{H-NMR}$ (DMSO- d_6) spectrum of **4** demonstrated a signal at δ 3.33 ppm for the protons of $\text{N}(\text{CH}_3)_2$ moiety. In **IR** spectrum of **5** showed a sharp band at

2210 cm^{-1} for CN group was appeared. $^1\text{H-NMR}$ (DMSO- d_6) results of compound **5** demonstrated triplet and quartet signals at δ 1.17 and 2.70 ppm corresponding to the protons of formimidate group. Also, **IR** spectrum of **6** exhibited two bands were observed at 3333 and 1647 cm^{-1} referring to NH and C=O groups. While $^1\text{H-NMR}$ (DMSO- d_6) spectrum of **6** revealed the existence of two signals at δ 1.03 and 1.23 ppm for the protons of two *p*- CH_3 groups on phenyl rings. $^{13}\text{C-NMR}$ (DMSO- d_6) of compound **1** revealed two characteristic signals at δ 126.14 and 169.13 ppm for CN and C=O groups, respectively. Also, $^{13}\text{C-NMR}$ (DMSO- d_6) data of compound **6** exhibited signals at δ 21.92 and 43.68 ppm for 2- PhCH_3 and SO_2CH_3 , respectively.

3.2 Biology

Antitumor activity of novel compounds **1-6** was screened against colon carcinoma (HCT-116), hepatic carcinoma (HepG-2) and breast carcinoma (MCF-7) cell lines adopting doxorubicin as a standard (**Table 2**). The majority of these compounds displayed weak cytotoxicity against

tested cancer cell lines. Conversely, compound **5** displayed equipotent activity to doxorubicin against HCT-116 (IC_{50} = 5.2 μ M) and promising action toward HepG-2 and MCF-7 with IC_{50} = 3.4 and 1.4 μ M in contrast to doxorubicin (IC_{50} = 2.85 and 1.03 μ M, respectively). Concerning structural activity relationship (SAR), it was noted that the weak potency was revealed by pyrano[3,2-*c*]pyridine-3-carbonitrile scaffold with acetamide in **2** and N,N-dimethylformimidamide in **4** or upon fusion with pyrimidinone moiety giving pyrido[3',4':5,6]pyrano[2,3-*d*]pyrimidin-4-ones **6**. A slight increase in the cytotoxicity was obtained upon substitution at position 2 of pyranopyridine moiety with chloroacetamide fragment in compound **3** (IC_{50} = 20.8 \neq HCT-116, 7.7 \neq HepG-2 and 4.5 \neq MCF-7 μ M). The excellent antiproliferative activity was yielded upon substitution at position 2 of pyranopyridine moiety with formimidate fragment in compound **5** (IC_{50} = 5.2 \neq HCT-116, 3.4 \neq HepG-2 and 1.4 \neq MCF-7 μ M).

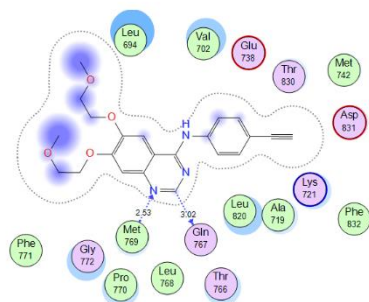
Table 2. IC_{50} of the test compounds **1-6** against HCT-116, HepG-2, and MCF-7 cancer cell lines at different concentrations.

Compound Code	IC_{50} (μ M) mean \pm SD		
	HCT-116	HepG-2	MCF-7
1	30.4 \pm 0.4	20.9 \pm 0.5	15.2
2	32.3 \pm 0.4	19.8 \pm 0.2	6.7 \pm 0.6
3	20.8 \pm 0.2	7.7 \pm 0.4	4.5 \pm 0.6
4	30.1 \pm 0.5	18.8 \pm 0.4	7.3 \pm 0.2
5	5.2 \pm 0.1	3.4 \pm 0.3	1.4 \pm 0.6
6	41.6 \pm 0.1	20.8 \pm 0.7	9.6 \pm 0.2
Doxorubicin	5.2 \pm 0.3	2.85 \pm 0.4	1.03 \pm 0.4

IC_{50} : Compound concentration required to inhibit the cell viability by 50 %, SEM = Standard error mean; each value is the mean of three values

3.3 Docking study

Using a docking technique, the binding mode of pyrano[3,2-*c*]pyridine derivative **5** was studied in



relation to the suggested targets EGFR [16] and VEGFR-2 [17] (PDB code: 1M17 and 4ASD, respectively) to postulate their mechanism of cytotoxicity. The co-crystallized ligands in the binding pocket served as a reference for docking of compound **5**. The native ligands erlotinib and sorafenib were re-docked to validate the docking method, yielding an RMSD value of 0.95 and 0.89, respectively. The binding mode of erlotinib with EGFR kinase (Figure 4) displayed that erlotinib occupies the ATP binding site where N1-quinazoline accepts hydrogen bond from Met769 (2.70 Å). Also, C2-quinazoline donated hydrogen bond to the backbone of Gln767. The results of docking investigation indicated that newly synthesized analogue **5** has good fitting and affinity for the examined targets (Table 3). As demonstrated in (figure 5), compound **5** established a hydrogen bond acceptor across sulphonyl oxygen and the backbone of Met769. Also, Asp831 located in the C-lobe accepted hydrogen bond from the ethyl group of formimidate moiety of compound **5**. Also, the backbone of Asp831 formed hydrogen bond donor with the N of CN group. In addition to that, CN group of compound **5** formed hydrogen bond acceptor with the side chain of Lys721. Phenyl ring of **5** formed arene-H interaction with Lys721 which also donated hydrogen bond to N-formimidate. On the other hand, sorafenib redocked into VEGFR-2 (PDB code: 4ASD) (Figure 6) showing that it fits well in the ATP binding site where the two N atoms of ureat moiety donated two hydrogen bonds to the side chain of Glu885. The oxygen atom of ureat moiety accepted hydrogen bond from the back bone of Asp1046 residue. Pyridine ring displayed arene-H interaction with Leu1035. The key amino acid Cys919 donated hydrogen bond to the N-pyridine and accept another one from the amide-N atom (distance = 3.22 and 2.76 Å, respectively).

Furthermore, Compound **5** formed hydrogen bond between formimidate moiety and the side chain of **Glu885** located in the ATP binding site of VEGFR-2 (figure 7). So, compound **5** showed better affinity to EGFR over VEGFR-2.

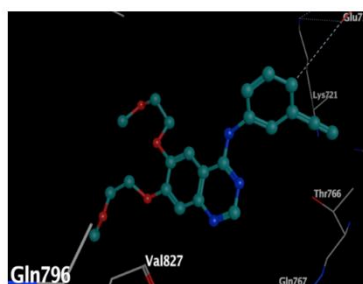


Figure 4. 2D&3D binding interaction of erlotinib with EGFR kinase (pdb code: 1M17).

Table 3. The docking binding free energies of erlotinib, sorafenib and the newly synthesized compound **5** against EGFR and VEGFR-2.

Compound	Binding free energy (kcal/mol)		Amino acid residues (bond length Å ⁰)	
	EGFR	VEGFR-2	EGFR	VEGFR-2
5	-6.60	-5.90	Asp831(3) Lys721(2.53) Met769(3.09)	Glu885(3.09) Arg1027(3.35)
erlotinib	-9.21	-	Met769 (2.70) Gln767 (3.02)	
sorafenib	-	-10.01		Glu885 (2.70 and 3.05) Asp1046 (2.83) Leu1035 Cys919

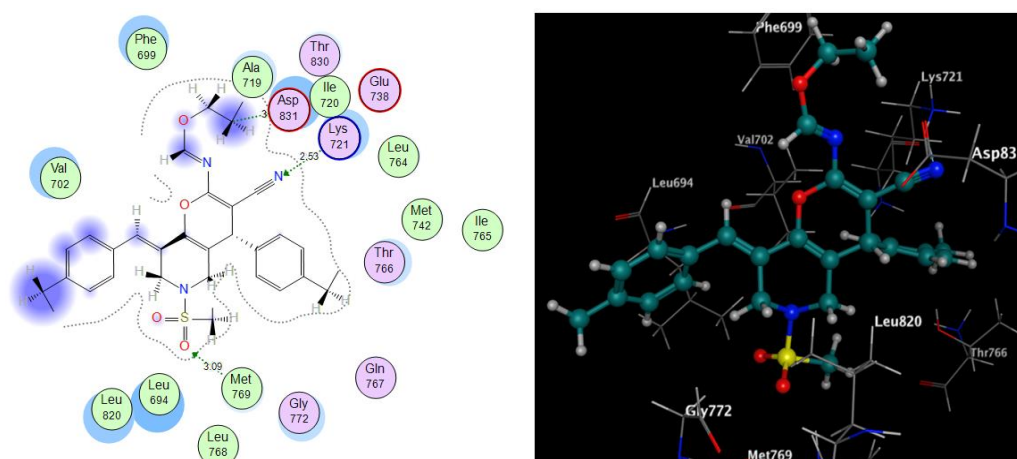


Figure 5. 2D and 3D of compound **5** into the active site of EGFR kinase.

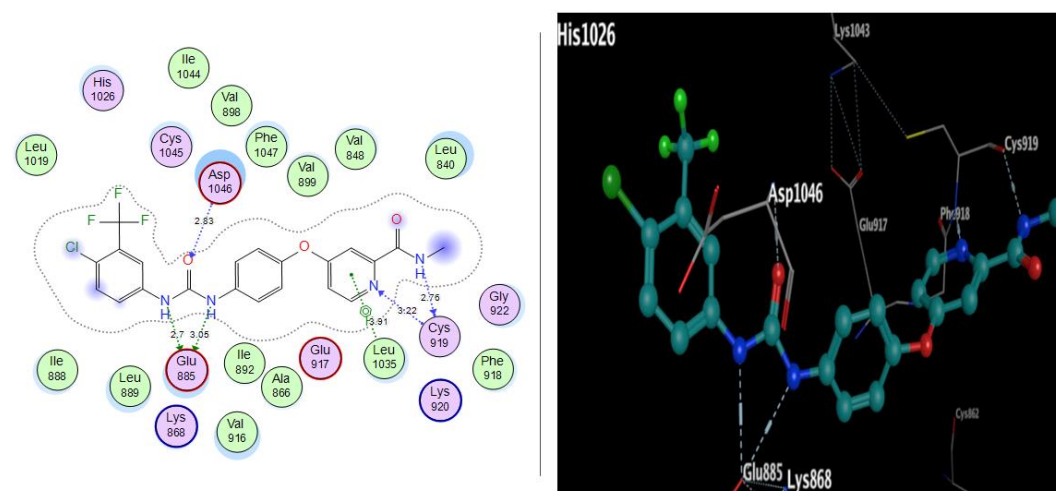


Figure 6. 2D&3D binding interaction of sorafenib with VEGFR-2 kinase (pdb code: 4ASD).

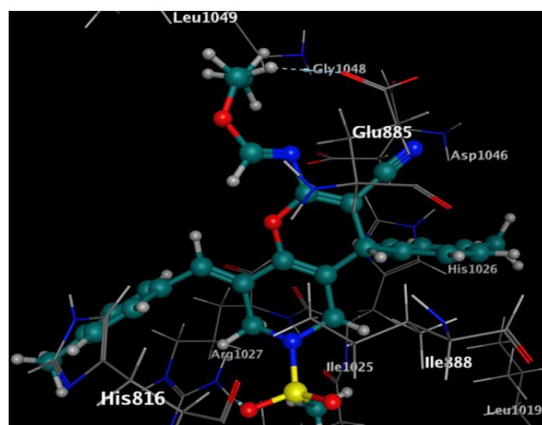
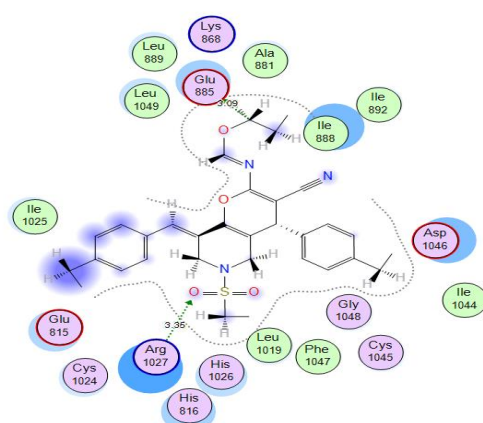


Figure 7. 2D and 3D of compound **5** into the active site of VEGFR-2.

5. CONCLUSIONS

Novel pyranopyridines **1-6** were designed, synthesized through reaction of NH_2 at **B** with ethyl cyanoacetate, acetic anhydride, chloroacetyl chloride, DMFDMA, triethyl orthoformate and formic acid. The newly synthesized compounds were assessed for their cytotoxicity against three cancer cell lines namely, colon carcinoma (HCT-116), hepatic carcinoma (HepG-2) and breast carcinoma (MCF-7) in contrast to doxorubicin. Chemical structures of **1-6** were established from its microanalytical and spectral data. Compound **5** exhibited significant cytotoxicity comparing to doxorubicin. Docking study was done versus EGFR kinase and VEGFR-2 (PDB code: 1M17 and 4ASD, respectively) to understand the proposed mechanism of their cytotoxic activity.

Funding: No funding.

Acknowledgments: The authors thank the National Research center for supporting this work.

Conflicts of Interest The authors declare no conflict of interest.

Author Contribution: All authors had full access to all the information and took responsibility for data integrity and data analysis accuracy. Authors Heba S. A. Elzahabi and Aladdin M. Srour designed the study. Author Safeya M. Mousa performed the experimental work. Authors Eman S. Nossier and Safeya M. Mousa wrote the manuscript. Author Hanem M. Awad performed the cytotoxic activity. Author Heba S. A. Elzahabi supervised the work and revised the whole manuscript. The final manuscript was read and accepted by all the contributors.

List of Abbreviations: EGFR: Epidermal growth factor receptor., VEGFR-2: Vascular endothelial growth factor receptor-2.

REFERENCES

1. Al-Warhi, Tarfah, et al. "Identification of Novel Cyanopyridones and Pyrido [2, 3-D] Pyrimidines as Anticancer Agents with Dual VEGFR-2/HER-2 Inhibitory Action: Synthesis, Biological Evaluation and Molecular Docking Studies." *Pharmaceuticals* 15.10 (2022): 1262-1284.
2. Padma, V. V. (2015). An overview of targeted cancer therapy. *BioMedicine*, 5, 1-6.
3. Du, Z., & Lovly, C. M. (2018). Mechanisms of receptor tyrosine kinase activation in cancer. *Molecular cancer*, 17, 1-13.
4. Salama, S. K., Mohamed, M. F., Darweesh, A. F., Elwahy, A. H., & Abdelhamid, I. A. (2017). Molecular docking simulation and anticancer assessment on human breast carcinoma cell line using novel bis (1, 4-dihydropyrano [2, 3-c] pyrazole-5-carbonitrile) and bis (1, 4-dihydropyrazolo [4', 3': 5, 6] pyrano [2, 3-b] pyridine-6-carbonitrile) derivatives. *Bioorganic Chemistry*, 71, 19-29.
5. Eissa, A. A., Aljamal, K. F., Ibrahim, H. S., & Allam, H. A. (2021). Design and synthesis of novel pyridopyrimidine derivatives with anchoring non-coplanar aromatic extensions of EGFR inhibitory activity. *Bioorganic Chemistry*, 116, 105318.
6. Avraham, R., & Yarden, Y. (2011). Feedback regulation of EGFR signalling: decision making by early and delayed loops. *Nature reviews Molecular cell biology*, 12(2), 104-117.
7. Al-Warhi, T., Sallam, A. A. M., Hameda, L. R., El Hassab, M. A., Aljaeed, N., Alotaibi, O. J. & Ibrahim, M. H. (2022). Identification of Novel Cyanopyridones and Pyrido [2, 3-D] Pyrimidines as Anticancer Agents with Dual VEGFR-2/HER-2 Inhibitory Action: Synthesis, Biological Evaluation

- and Molecular Docking Studies. *Pharmaceuticals*, 15(10), 1262.
8. Yousef, R. G., Elkady, H., Elkaeed, E. B., Gobaara, I. M., Al-Ghulikah, H. A., Husein, D. Z. & Eissa, I. H. (2022). (E)-N-(3-(1-(2-(4-(2, 2-Trifluoroacetamido) benzoyl) hydrazono) ethyl) phenyl) nicotinamide: A Novel Pyridine Derivative for Inhibiting Vascular Endothelial Growth Factor Receptor-2: Synthesis, Computational, and Anticancer Studies. *Molecules*, 27(22), 7719.
9. Mungra, D. C., Patel, M. P., Rajani, D. P., & Patel, R. G. (2011). Synthesis and identification of β -aryloxyquinolines and their pyrano [3, 2-c] chromene derivatives as a new class of antimicrobial and antituberculosis agents. *European journal of medicinal chemistry*, 46(9), 4192-4200.
10. Chen, C., Lu, M., Liu, Z., Wan, J., Tu, Z., Zhang, T., & Yan, M. (2013). Synthesis and evaluation of 2-amino-4H-pyran-3-carbonitrile derivatives as antitubercular agents. *Open Journal of Medicinal Chemistry*, 3(04), 128.
11. Al-Warhi, T., Al-Karmalawy, A. A., Elmaaty, A. A., Alshubramy, M. A., Abdel-Motaal, M., Majrashi, T. A. & Sharaky, M. (2023). Biological evaluation, docking studies, and in silico ADME prediction of some pyrimidine and pyridine derivatives as potential EGFRWT and EGFR790M inhibitors. *Journal of Enzyme Inhibition and Medicinal Chemistry*, 38(1), 176-191.
12. Nagasundaram, N., Padmasree, K., Santhosh, S., Vinoth, N., Sedhu, N., & Lalitha, A. (2022). Ultrasound promoted synthesis of new azo fused dihydropyrano [2, 3-c] pyrazole derivatives: In vitro antimicrobial, anticancer, DFT, in silico ADMET and Molecular docking studies. *Journal of Molecular Structure*, 1263, 133091.
13. Al-Warhi, T., Sallam, A. A. M., Hemedat, L. R., El Hassab, M. A., Aljaeed, N., Alotaibi, O. J., & Ibrahim, M. H. (2022). Identification of Novel Cyanopyridones and Pyrido [2, 3-D] Pyrimidines as Anticancer Agents with Dual VEGFR-2/HER-2 Inhibitory Action: Synthesis, Biological Evaluation and Molecular Docking Studies. *Pharmaceuticals*, 15(10), 1262.
14. Nagasundaram, N., Padmasree, K., Santhosh, S., Vinoth, N., Sedhu, N., & Lalitha, A. (2022). Ultrasound promoted synthesis of new azo fused dihydropyrano [2, 3-c] pyrazole derivatives: In vitro antimicrobial, anticancer, DFT, in silico ADMET and Molecular docking studies. *Journal of Molecular Structure*, 1263, 133091.
15. Thanh, N. D., Giang, N. T. K., Ha, N. T. T., Le, C. T., Van, H. T. K., & Toan, V. N. (2023). Synthesis and in vitro anticancer activity of 4H-pyrano [2, 3-d] pyrimidine-1H-1, 2, 3-triazole hybrid compounds bearing D-glucose moiety with dual EGFR/HER2 inhibitory activity and induced fit docking study. *Journal of Molecular Structure*, 1271, 133932.
16. Saleh, N. M., Abdel-Rahman, A. A. H., Omar, A. M., Khalifa, M. M., & El-Adl, K. (2021). Pyridine-derived VEGFR-2 inhibitors: rational design, synthesis, anticancer evaluations, in silico ADMET profile, and molecular docking. *Archiv der Pharmazie*, 354(8), 2100085.
17. Fawzy, N. G., Panda, S. S., Fayad, W., El-Manawaty, M. A., Srour, A. M., & Girgis, A. S. (2019). Novel curcumin inspired antineoplastic 1-sulfonyl-4-piperidones: design, synthesis and molecular modeling studies. *Anti-Cancer Agents in Medicinal Chemistry (Formerly Current Medicinal Chemistry-Anti-Cancer Agents)*, 19(8), 1069-1078.
18. Srour, A. M., Nossier E. S., Mousa, S. M. ^b, Awad, H. M., Elzahabi, H. S. A. (2024). New Pyrano-Pyridine Conjugates as Potential Anticancer Agents: Design, Synthesis and Computational Studies. *Future Medicinal Chemistry*, in press.
19. Thabrew, M. I., Hughes, R. D., & McFarlane, I. G. (1997). Screening of hepatoprotective plant components using a HepG2 cell cytotoxicity assay. *Journal of pharmacy and pharmacology*, 49(11), 1132-1135.
20. Gaber, A. A., Bayoumi, A. H., El-Morsy, A. M., Sherbiny, F. F., Mehany, A. B., & Eissa, I. H. (2018). Design, synthesis and anticancer evaluation of 1H-pyrazolo [3, 4-d] pyrimidine derivatives as potent EGFRWT and EGFR790M inhibitors and apoptosis inducers. *Bioorganic chemistry*, 80, 375-395.
21. Stamos, J., Sliwkowski, M. X., & Eigenbrot, C. (2002). Structure of the epidermal growth factor receptor kinase domain alone and in complex with a 4-anilinoquinazoline inhibitor. *Journal of biological chemistry*, 277(48), 46265-46272.
22. Okamoto, K., Ikemori-Kawada, M., Jestel, A., von König, K., Funahashi, Y., Matsushima, T. & Matsui, J. (2015). Distinct binding mode of multikinase inhibitor lenvatinib revealed by biochemical characterization. *ACS medicinal chemistry letters*, 6(1), 89-94.